

OPEN ACCESS

EDITED BY Natalia Szejko, Medical University of Warsaw, Poland

REVIEWED BY

Katarzyna Smilowska, Radboud University Medical Centre, Netherlands Mariam Hull, Texas Children's Hospital, United States

*CORRESPONDENCE Makoto Miyakoshi

Makoto.Miyakoshi@cchmc.org

ACCEPTED 16 August 2025
PUBLISHED 28 October 2025

CITATION

Miyakoshi M, Jurgiel J, Dillon A, Piacentini J, Makeig S and Loo SK (2025) EEG power modulation in the sensorimotor regions is critical to motor tic suppression. Front. Psychiatry 16:1580636. doi: 10.3389/fpsyt.2025.1580636

COPYRIGHT

© 2025 Miyakoshi, Jurgiel, Dillon, Piacentini, Makeig and Loo. This is an open-access article distributed under the terms of the Creative Commons Attribution License (CC BY). The use, distribution or reproduction in other forums is permitted, provided the original author(s) and the copyright owner(s) are credited and that the original publication in this journal is cited, in accordance with accepted academic practice. No use, distribution or reproduction is permitted which does not comply with these terms.

EEG power modulation in the sensorimotor regions is critical to motor tic suppression

Makoto Miyakoshi^{1,2,3}*, Joseph Jurgiel⁴, Andrea Dillon⁴, John Piacentini⁴, Scott Makeig³ and Sandra K. Loo⁴

¹Division of Child and Adolescent Psychiatry, Cincinnati Children's Hospital Medical Center, Cincinnati, OH, United States, ²Department of Psychiatry and Behavioral Neuroscience, University of Cincinnati College of Medicine, Cincinnati, OH, United States, ³Swartz Center for Computational Neuroscience, Institute for Neural Computation, University of California San Diego, La Jolla, CA, United States, ⁴Semel Institute for Neuroscience and Human Behavior, University of California, Los Angeles, CA, United States

Background: The neural mechanisms underlying tic suppression in chronic tic disorder (CTD) have been investigated using various neuroimaging modalities. A limitation in studying CTD is that abrupt motor action is inherent to the nature of the disorder, but the movement makes any form of neural recording challenging. However, recent advances in hardware and software technologies have enabled EEG studies during motion, which open new avenues for studying CTD with EEG. **Methods:** We performed an event-related EEG power spectral analysis in children with chronic tic disorder (CTD) or typically developing children (TDC) as controls in a sample of 76 children (39 CTD) contributing to the final statistics. There were three block-separated conditions: no suppression (NoSupp), suppression with verbal instruction (Supp_{Vrb}), and suppression with reward (Supp_{Rwd}); the latter two conditions were collapsed into Supp_{Ave}. EEG data were processed using independent component analysis, and the event-related potential was decomposed in the time-frequency domain.

Results: During tic or blink suppression, both CTD and TDC showed EEG power increase centered within the theta range in frontal, cingulate, and central regions. Meanwhile, the CTD group showed the opposite pattern in broadband EEG power modulation relative to controls, particularly in the centro-temporal sensorimotor regions. The regression analysis between this broadband power and tic suppression performance resulted in a significant positive correlation.

Conclusions: Better tic suppression was associated with increased EEG power, a similar pattern observed among controls during blink suppression. EEG power in sensorimotor regions is a neural marker of tic suppression performance in children with CTD.

KEYWORDS

chronic tic disorder (CTD), EEG, children, blink, suppression (psychology)

Highlights

 Children with chronic tic disorder (CTD) performed a tic suppression task. We did not replicate the expected effect of the use of reward for enhancing the suppression.

- We recorded pre-tic brain dynamics and analyzed them using a high-density EEG recording system with advanced signal processing techniques to address the issue of ticrelated artifacts.
- We found performance of tic suppression is associated with an increase in EEG power in the right post-central and the left mid-temporal EEG sources.

Introduction

Tics are defined by sudden, involuntary, and recurrent movements or vocalizations found in children with Chronic Tic Disorders (CTD) including Tourette syndrome. CTD behavior is considered to be related to deficits in motor inhibition and also top-down control. Tics can usually be voluntarily delayed or inhibited on demand, but the neural correlates of this process are still under investigation. A recent meta-analysis found general but inconsistent inhibitory deficits in CTD relative to typically developing controls, in which the effect size varied by task with commonly used inhibitory paradigms include Stop Signal, Flanker, and Go/No-go tasks (1). Clarifying the neural mechanisms of suppression in CTD is important to understand how mental effort controls behavior, and will have critical value in child psychiatry, for example, in designing a clinical behavioral training program for treating children with Tourette's syndrome.

Neuroimaging studies have shown that the sensorimotor cortex is involved in both the generation and voluntary inhibition of tics. Altered limbic input to the sensorimotor cortex and abnormal GABA-mediated beta-band oscillations measured with magnetoencephalography (MEG) have been detected in the sensorimotor cortex and are suggested to be related to disturbances in sensorimotor processing that may contribute to tic generation (2). Studies using transcranial magnetic stimulation (TMS) have suggested that the primary motor cortex is an important relay in the tic generation circuit, and children with greater tic severity have less excitable motor cortices at rest, possibly as a result of adaptations to suppress unwanted movements (3-5). For the voluntary inhibition of tics, the involvement of the prefrontal cortex has been reported. Regional homogeneity of the blood-oxygen-level dependent (BOLD) signals within the relatively small anatomically defined region within the left inferior frontal gyrus increased in proportion to the CTD children's ability to inhibit their tics (6). Patients with CTD exhibit increased activation in the direct pathway through the basal ganglia and prefrontal cortex as well as the subthalamic nucleus as compensatory

Abbreviations: CTD, chronic tic disorder; ICA, independent component analysis; ERSP, event-related spectral perturbation.

activations (7). These neuroimaging results have high spatial resolution and provide detailed anatomical information related to CTD. However, both positron emission tomography (PET) and magnetic resonance (MR) imaging have general limitations, such as severely affected signal quality due to body movement during scans, and the time course of BOLD changes being on the order of seconds, likely much slower than the timing of neural phenomena. How the intrinsic environment of MR imaging interacts with CTD and its impact on the time resolution of tic events remains unknown. To avoid these limitations in MR imaging, scalp-recorded EEG provides a good alternative.

There are several EEG studies during tic suppression. Prominent increases in theta oscillation in the prefrontal area were observed during tic suppression (8). These authors also reported an increase in partial directed coherence in the frontomotor regions in the theta and beta bands. Elevated alpha coherence was found between sensorimotor areas and the prefrontal and mesial frontal cortex during the suppression of tics (9). However, a decrease in frontotemporal/occipital/parietal connectivity during rest was also reported (10), making the interpretation of the connectivity results somewhat inconsistent. Another study reported employment of the default mode network during tic suppression within the alpha band (11). These EEG studies, as well as most neuroimaging studies, adopted a block design. This is because tic causes body movements that by definition need to be removed from the data analysis, although the target event is the tic itself. Another reason is that EEG research has largely relied on the presence of pre-defined event-related potential (ERP) components, such as P300. In order to fully exploit the richness of high-resolution temporal dynamics of EEG, applying event-related spectral power analysis in the time-frequency domain is desirable. However, event-related EEG analysis targeting the pre-tic interval in children with CTD has not been attempted. An exception is a study reporting peri-tic EEG modulation in adults with CTD (12). However, this pioneering work suffers from poor time-frequency resolution in the result and low validity of in the interpretation of the EEG modulation during tic.

The purpose of the current study is to compare the timefrequency dynamics of event-related EEG during tic and blink suppression between CTD and TDC. This is the first study reporting modulations in broad-band EEG power spectrum during voluntary tic suppression in children with chronic tic disorder. There are two EEG studies on voluntary tic suppression (11, 13), but none of them reported broad-band EEG power modulations in a pediatric cohort. EEG power modulation better translates to localized BOLD signal modulations during tic suppression paradigm (14-16) than phase-based connectivity analysis (11). We expected that the right anterior prefrontal cortex would show power increase based on the previous fMRI studies on tic suppression (16), blink suppression (17), as well as general response inhibition paradigm (18, 19). Our time window of interest is the -5 to 0 seconds prior to the tic or blink event. This approach helps minimize contamination from artifacts caused by body movements. Our group has already established a dedicated signal processing pipeline and has validated its effectiveness with

control children (20). Utilizing blink suppression in TDC as an analogue for tic suppression in CTD is an accepted method for studying involuntary movements (16, 21). While eye blinks are a natural phenomenon, they also represent one of the most frequently reported tics (22). Blink suppression paradigms have proven effective for examining the neural correlates of urges in control subjects (17). Finally, we also explored the impact of reward on suppression, as previous research has indicated that reward can enhance successful tic suppression (23, 24). In our earlier study, we found that reward enhanced blink suppression in TDC (20) and we aimed to replicate this finding regarding tic suppression in CTD.

Methods

Ethical compliance

The Internal Review Board Committee of the University of California, Los Angeles, approved the current study (IRB number 13 - 00538). The study was conducted in accordance with the provisions of the Declaration of Helsinki. All participants submitted written informed consent. Prior to analysis, we removed participants' personal information from the data to ensure their de-identification.

Samples

The children were recruited from the community through social media advertisements, community organizations, and local schools, as well as from the academic medical clinics through primary care physicians and local clinicians. After receiving verbal and written explanations of study requirements, and prior to any study procedures, all parents/participants provided written permission and assent as approved by the Institutional Review Board. A total of 115 children were recruited. In the current study, we focused on those who showed a minimum of 15 tics and blinks during sessions. A subset of 76 children, including 37 typically developing children (TDC, 19 males, mean age 9.6, SD 1.4, range 8 - 12) and 39 children with tic disorder (CTD, 27 males, mean age 9.7, SD 1.6, range 8 - 14), was included in the current study. There was 1 child in CTD comorbid with ADHD on stimulants who was asked to discontinue 24 hours prior to coming into the lab, and 9 children on other psychotropic medicines. The demographic data of this subset is summarized in Table 1.

Procedures

All participants underwent diagnostic interviews and EEG recording. Psychiatric diagnoses were determined using a semi-structured diagnostic interview, either the Anxiety Disorder Interview Schedule, Child Version (ADIS) (25), modified to cover Tourette and other tic disorders or the KSADS (26) and administered by graduate or doctoral level psychologists. The ADIS and KSADS were supplemented by the clinician-administered Yale Global CTD

TABLE 1 Demographics and clinical characteristics of participants for the EEG study.

Demographics	TDC	CTD
N	37	39
Age, M (SD)	9.6 (1.5)	9.7 (1.6)
Sex, males, N (%)	19 (51%)	27 (69%)
Full Scale IQ, M (SD)	116 (15)	111 (15)
Clinical Characteristics		
ADHD, N (%)	0 (0%)	23 (59%)
OCD, N (%)	0 (0%)	17 (44%)
Generalized anxiety disorder, N (%)	0 (0%)	12 (31%)
No comorbidities, N (%)	37 (100%)	9 (23%)
YGTSS, M (SD)		
Total score	0 (0)	29.4 (7.7)
Impairment	0 (0)	28.5 (7.9)
PUTS, M (SD)		
Urge presence	N/A	4.7 (2.3)
Urge strength	N/A	4.6 (2.3)
Tic frequency	N/A	5.3 (2.0)
CBCL total, M (SD)	42.0 (9.4)	59.6 (10.3)
SWAN, M (SD)		
Inattention	32.5 (8.5)	23.6 (9.4)
Hyperactivity	32.5 (9.6)	25.6 (9.0)
CYBOCS, M (SD)	N/A	10.0 (10.7)
Medication		
No medication, N (%)	39 (100.0)	29 (74.4)
Stimulant, N (%)	0 (0)	1 (2.6)
Psychotropic, N (%)	0 (0)	9 (23.1)
α -2 agonist	0 (0)	5 (12.8)
Antidepressant	0 (0)	5 (12.8)
Anticonvulsant	0 (0)	1 (2.6)
Antipsychotic	0 (0)	1 (2.6)
Antihypertensive	0 (0)	1 (2.6)
Manage CD at a first facilities IO in the		

M, mean; SD, standard deviation; IQ, intelligence quotient; ADHD, attention-deficit/hyperactivity disorder; OCD, obsessive-compulsive disorder; YGTSS, Yale Global Tic Severity Scale; PUTS, Premonitory Urge for Tics Scale; CBCL, Child Behavior Checklist; SWAN, Strengths and Weaknesses of ADHD-symptoms and Normal-behavior scale; CYBOCS, Child Yale-Brown Obsessive-Compulsive Scale. N/A, Not Available.

Severity Schedule (YGTSS) (27), Child Yale-Brown Obsessive-Compulsive Scale (CYBOCS) (28), and Premonitory Urge for CTDs Scale (PUTS) (29). Symptoms of ADHD were measured using the Strengths and Weaknesses of ADHD-symptoms and Normal-behavior (SWAN) scale (30). To assess and quantify broad-band behavioral functioning, parents completed the Child

Behavior Checklist (CBCL) (31) and the Behavior Rating of Individual Executive Functions (BRIEF) (32). Senior clinicians (JP, SC, AD) confirmed the presence of DSM - 5 psychiatric diagnoses after an individual review of each participant's symptoms, duration, and impairment level. Estimated intelligence (IQ) was assessed using the Wechsler Abbreviated Scale of Intelligence (WASI) (33). Subjects were excluded from participation if they were positive for any of the following: head injury resulting in a concussion, diagnoses of autism, major depression, bipolar disorder, panic disorder or psychosis, estimated Full Scale IQ < 80 or YGTSS <15 (CTD only). In addition, TDC subjects were excluded if they had any major Axis I diagnosis or were on any type of psychoactive medication.

Task

There were three block-separated conditions: tic or blink freely i.e., no suppression (NoSupp), verbal instruction for blink suppression (Supp $_{\rm Vrb}$), and blink suppression for reward (Supp $_{\rm Rwd}$). All children were instructed to tic or blink freely during the NoSupp block, while trying to suppress tics/blinks during the two suppression blocks. During Supp $_{\rm Rwd}$, children were told that the computer would be counting how many tics/blinks they were able to suppress, and that they would subsequently receive a reward for successful suppression. All children received \$10 regardless of how many tics or blinks they exhibited. The order of the three conditions was counterbalanced across subjects. Each block length was between 5 – 7 min. This variability is due to the update of the experimental protocol in the middle of the project.

Identifying tics and blinks

For annotating tics, we used the video recordings that were timestamp-synchronized to EEG and other data streamed by LSL to identify the onset of the tics. There was a single rater to annotate tic onset markers. For annotating blinks, we developed an EEGLAB plugin called <code>countBlinks()</code> for this project (available from https://sccn.ucsd.edu/eeglab/plugin_uploader/plugin_list_all.php) to manually annotate all the blinks during the tasks by visually examining the time-series data of the independent component (IC) representing blink/vertical eye movement. For a detailed description and validation of this program, see Miyakoshi et al. (20).

EEG recording

EEG signals were recorded using the Electrical Geodesics Incorporated (EGI) hardware and software with 128 Hydrogel electrodes embedded in a hydrocel net in an International 10/10 location system. The data were sampled at 1000 Hz and initially referenced to Cz. The electrode-skin impedance threshold was set at 50 kOhms per the manufacturer's standard for the high input impedance amplifier. Eye movements were monitored by electrodes placed on the outer canthus of each eye for horizontal movements (REOG, LEOG)

and by electrodes above the eyes for vertical eye movements. Facial electromyography (EMG) leads were placed on the cheeks bilaterally over the zygomaticus major muscles to assist with the detection of facial movements. Key head landmarks (nasion, inion, preauricular notches) and 3-D electrode locations were recorded (Polhemus, Inc.) to allow for the reconstruction of electrode positions on the scalp. All EEG data were recorded using the Lab Streaming Layer (LSL, https://github.com/sccn/labstreaminglayer), which allowed for the integration of multiple data streams including EEG, high-definition video, and experimental events.

EEG preprocessing

Throughout the preprocessing, we used EEGLAB 14.1.2 (34) running under Matlab 2017b (The MathWorks, Inc., Natick, MA, USA). Custom code was written as necessary. There were two central signal processing techniques: artifact subspace reconstruction (ASR) (35-41), which is an offline version of data cleaning suits from BCILAB (42), and independent component analysis (ICA) (43-46). The details of the method can be found in our previous publication (20). These two approaches are complementary in that ASR uses sliding-window principal component analysis (PCA)-based subspace rejection and reconstruction so that it can address data nonstationarity such as infrequent short-lasting bursts by touching electrodes, for example, while ICA can find stationary processes and temporally maximally independent sources such as brain EEG sources as well as non-brain artifact sources like blink, eye movement, and facial and neck muscle activation by using more sophisticated, physiologically valid assumptions than PCA (47, 48). For each of the obtained independent components (IC), an equivalent current dipole model was fitted using Fieldtrip function dipfit3.3 (49) and fitTwoDipoles (50). The obtained ICs were also automatically annotated by ICLabel (51) to preselect only ICs labeled as 'Brain'. The mean rate of electrode rejection rate was 2.8% (SD 1.9, range 0 -9.4) and 5.3% (SD 2.1, range 4.1 - 16.4) for control and children with tic, respectively. The mean datapoint rejection rate was 0.67% (SD 2.1, range 0 - 11.4) and 0.4% (SD 0.9, range 0 - 4.1) for control and children with tic, respectively. After performing the IC rejection, the average number of ICs submitted to the final analysis was 48.4 (SD 11.2, range 16 - 68) and 40.1 (SD 13.0, range 18 - 65) for control and children with tic, respectively.

Group-level analysis

The prototype of the EEGLAB plugin *Eyen* was used to perform the following group-level analysis. A total of 3470/9312 ICs (37.3%) with a 'Brain' label were collected from the preselected 76 participants and submitted to k-means clustering using the dipole locations. The Silhouette Index (52) determined that the optimum number of clusters was 13. We analyzed event-related spectral perturbation (ERSP) on each anatomically associated IC cluster to investigate time-frequency-space decomposed EEG power dynamics related to tic or blink suppression.

Statistical testing

For the behavioral data analysis, the factorial design for the tic or blink count analyses was 2 (Groups: CTD and TDC) x 3 (Suppression Conditions: NoSupp, Supp $_{\rm Vrb}$, Supp $_{\rm Rwd}$). A paired ttest was performed across all the pairs of Suppression Conditions within each Group. Because the behavioral difference between Supp $_{\rm Vrb}$ and Supp $_{\rm Rwd}$ failed to show significance, we collapsed these conditions into a single Supp $_{\rm Ave}$ condition in the following analyses. To study the relationship between premonitory urges and tic frequency, we conducted correlation analyses between PUTS scores and normalized tic frequencies in NoSupp and Supp $_{\rm Ave}$ conditions.

For the EEG data analysis, the factorial design was reduced to 2 (Groups: CTD and TDC) x 2 (Suppression Conditions: NoSupp and Supp_{Ave}). A mixed design ANOVA was performed on each timefrequency cell of the calculated ERSP tensor with the dimensions of 50 (logarithmically spaced frequency bins, 1 to 50 Hz) x 1251 (latency to tic or blink, -5000 to 0 ms) x number_of_ICs (this varies from IC cluster to cluster) for 13 IC clusters. For the multiple comparison correction for the 50 x 1251 time-frequency points, weak family-wise error rate (wFWER) control was used (53). Fstatistics values were computed for all time-frequency points and thresholded at p < 0.05. The true mass of the cluster, which is the sum of absolute F-statistics within a time-frequency pixel cluster, was computed for each time-frequency pixel cluster separately. Next, the data labels were shuffled and the same procedure was applied, and the largest mass of the cluster was taken to build a distribution of surrogate mass of cluster. Finally, the 95th percentile of the surrogate mass of the cluster distribution was obtained to determine the threshold value for omnibus correction. Those true mass-of-cluster entries that were larger than the threshold value were declared to be statistically significant after wFWER control.

In order to study the relationship between behavioral performance in suppression and EEG power modulation, the suppression ratio was defined and calculated for all participants.

Supression Ratio =
$$NoSupp/((Supp_{Vrb} + Supp_{Rwd})/2)$$

We calculated the linear correlation between Δ ERSP, which is defined as the ERSP difference (Supp_Vrb + Supp_Rwd)/2 – NoSupp, and the Suppression Ratio for each IC cluster. When multiple ICs were associated with a single subject, the mean value was calculated across the ICs. To obtain the variance of this correlation, a bootstrap test was performed using the Matlab bootstrp() function with 2000 iterations on Δ ERSP, and the linear correlation against the Suppression Ratio was calculated. In addition, we also conducted correlation analyses between Δ ERSP and PUTS scores to examine the relationship between pre-tic EEG modulations and premonitory urges.

Finally, dipole density was generated by convolving a 3-D Gaussian smoothing kernel with FWHM = 20 mm. The Talairach atlas was used to determine the three highest associated anatomical labels (54, 55).

To control for the effects of age and drug (any psychotropic drug other than stimulants, which were discontinued 24 hours prior to testing), we utilized a linear mixed effect model (LME) implemented in Matlab using the fitlme() function. The formulae used for testing for group differences in the blink/tic counts and EEG power, as well as the within-group regression analysis between tic suppression score and EEG power, respectively, were as follows

Counts of blinks/tics or EEG power

= Age + Drug + Condition*Group

EEG power = Age + Drug + Suppression Score

where EEG power represents a numerical vector containing EEG's ERSP power within the statistically significant masks in the time-frequency domain, Age is a numerical vector indicating the participants' ages at the time of recording, Drug is a categorical variable denoting the use of psychotropic medication, Conditions is a categorical variable consisting of {NoSupp, Supp_{Nvd}}, and Group is a categorical vector comprising {CTD, TDC}. All of these were fixed effect variables. We did not include random effect variables for adopting the same fixed-effect statistics between behavioral and EEG data. Applying an LME model including a random effect for all time-frequency calculations would take 40.6 days to finish based on our estimation, which was not practical. We did, however, test the random intercept in the behavioral data: a likelihood-ratio test comparing the fixed-only model with a mixed model ($\sigma = 3.63$, $\Delta \chi^2 = 65.9$, df = 1, p = 4.4×10^{-16}) showed a better fit but did not change any significance decisions. Hence the simplified model is inferentially equivalent while remaining computationally feasible. We reported uncorrected p-values for these tests.

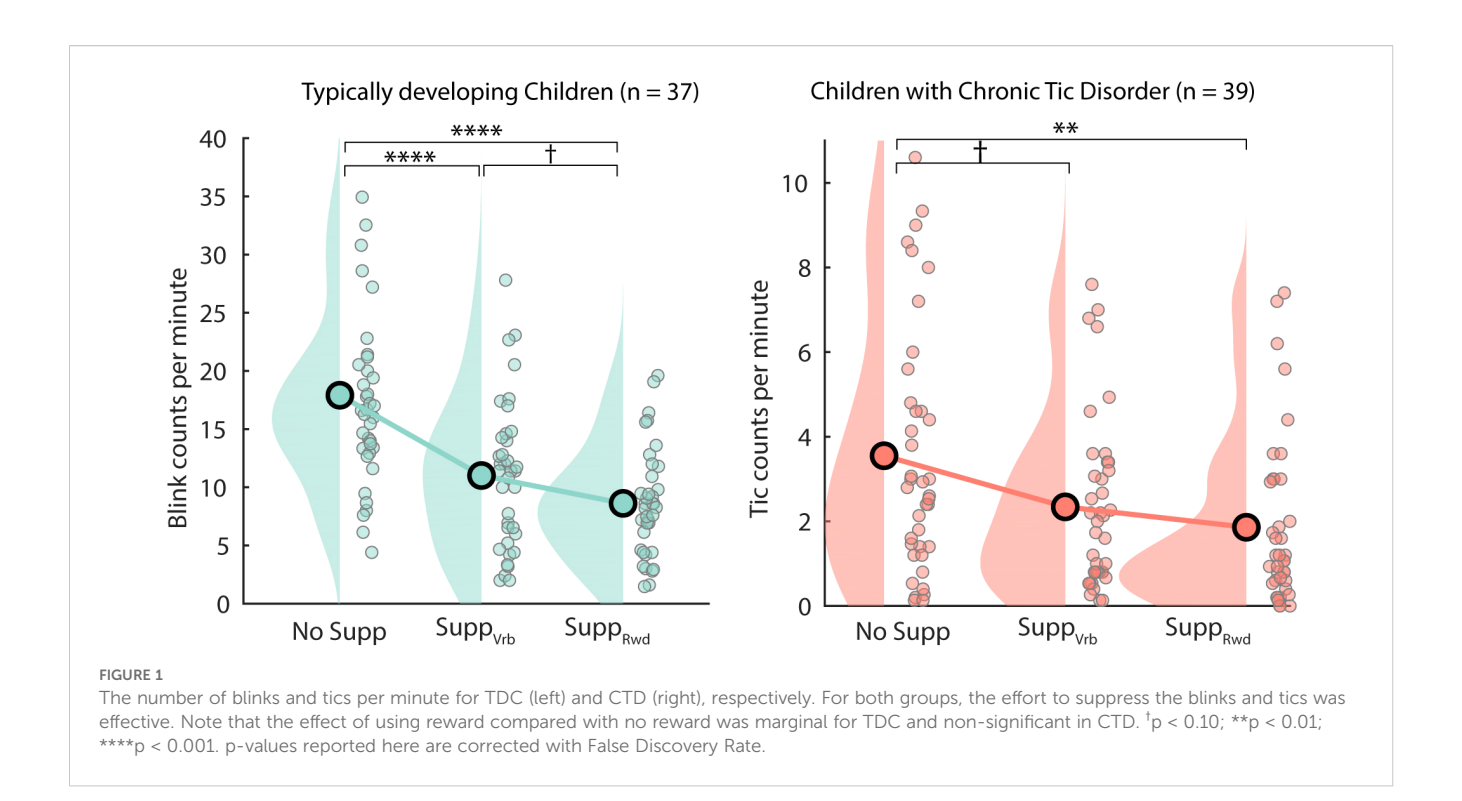
Results

Demographics

Demographic data for the primary study sample as well as the classifier test sample are described in Table 1. The primary sample displayed moderate tic severity with a mean total YGTSS score of 29.4 \pm 7.7. Comorbidities of ADHD, OCD, or an anxiety disorder were present in 77% of participants, as is typical for such populations.

Behavioral data

The numbers of tics and blinks were counted for each block and normalized into average counts per minute for each subject. The results are shown in Figure 1. For TDC, NoSupp, M = 17.9 (SD 8.8, range 4.4 - 48.6); Supp $_{\rm Vrb}$, M = 11.0 (SD 6.3, range 2 - 27.8); Supp $_{\rm Rwd}$, M = 8.6 (SD 4.7, range 1.5 - 19.6). For CTD, NoSupp, M = 3.6 (SD 2.9, range 0.1 - 10.6); Supp $_{\rm Vrb}$, M = 2.3 (SD 2.0, range 0.1 - 7.6); Supp $_{\rm Rwd}$, M = 1.9 (SD 2.0, range 0 - 7.4). The planned comparisons revealed significant differences between NoSupp $_{\rm VS}$. Supp $_{\rm Rwd}$ for both groups, both $_{\rm T}$ (72) and $_{\rm T}$ (76) > 2.99 for TDC and CTD, respectively, all $_{\rm T}$ $_{\rm T$



between NoSupp vs. Supp $_{\rm Vrb}$ were significant for TDC, t (72) = 3.88, P < 0.001, but it was marginal for CTD, t (76) = 2.12, P = 0.056. The difference between Supp $_{\rm Vrb}$ vs. Supp $_{\rm Rwd}$ was marginal for TDC, t (72) = 1.85, P = 0.082, and non-significant in CTD, t (76) = 1.05, p = 1. Because the behavioral results did not confirm the clear difference between Supp $_{\rm Vrb}$ vs. Supp $_{\rm Rwd}$, these two conditions were collapsed hereafter.

In order to assess the impact of Age and Drug on the result, we conducted LME modeling and included Age and Drug as fixed effect variables. The goodness of fit was evaluated using R^2 . The adjusted R^2 was 0.526. Neither Age nor Drug showed any significant impact (p = 0.649 and 0.912, respectively), while all other factors and the interaction term were found to be significant ($p < 2.81 \times 10^{-6}$). We conclude that Age and Drug cannot be dominant factors in the behavioral data.

The correlation analyses between PUTS scores and the normalized tic counts in NoSupp and Supp_{Ave} conditions, as well as the difference NoSupp - Supp_{Ave}. None of the tests reached statistical significance: R = 0.158 (p = 0.181), R = 0.147 (p = 0.214), and R = 0.055 (p = 0.643), respectively. Thus, our data did not support the prediction that premonitory urge correlates with tic severity (56).

EEG data: general description

37 TDC datasets showed an average of 48.4 ICs (SD 11.2, range 16 - 68), while 39 CTD datasets showed an average of 40.1 ICs (SD 13.0, range 18 - 65). The Silhouette algorithm determined the optimum number of k-means clusters as 13 (52). The mean number of TDC datasets and ICs per cluster is 34.8 (SD 2.1,

range 30 - 37) and 142.3 (SD 36, range 84 - 198), respectively, and for CTD datasets, it is 35.9 (SD 4.1, range 24 - 39) and 124.6 (SD 35.5, range 51 - 181).

EEG data: main effect suppression

Out of the 13 IC clusters, 4 of them showed the main effect of Suppression, including 2 frontal clusters (Figure 2). These frontal IC clusters, Mid Frontal R and Superior Frontal L, are characterized by the long-lasting theta-band power increase for Supp that started -3 to -2 s before the blink/tic onset. Our previous study reported frontal EEG power increase during blink suppression in typically developing children (20). The current result confirms that the same frontal EEG power increase also occurs in the CTD population during tic suppression. The result also confirms the view that blink suppression can be an analogue of tic suppression in terms of the frontal EEG power modulation. We also found that the Mid Cingulate IC cluster also showed the similarly extended pre-blink/tic power EEG power increase occurred in both groups, indicating functional correlation.

Note that the current dipole density of the Mid Cingulate IC cluster covering midbrain regions is physiologically implausible as a current source for the EEG signals. These deep current dipole models are results of the depth bias in fitting a *single* dipole model to a scalp topography contributed by a broad dipole *layer*. A typical dipole layer consists of a massive parallel array of micro dipoles that covers substantial (> 6.45 cm²) area of the cortical surface (57). The impact of Age and Drug was evaluated using the LME model including Age and Drug as fixed effect variables. For all the IC clusters shown in Figure 2, the main effect Suppression

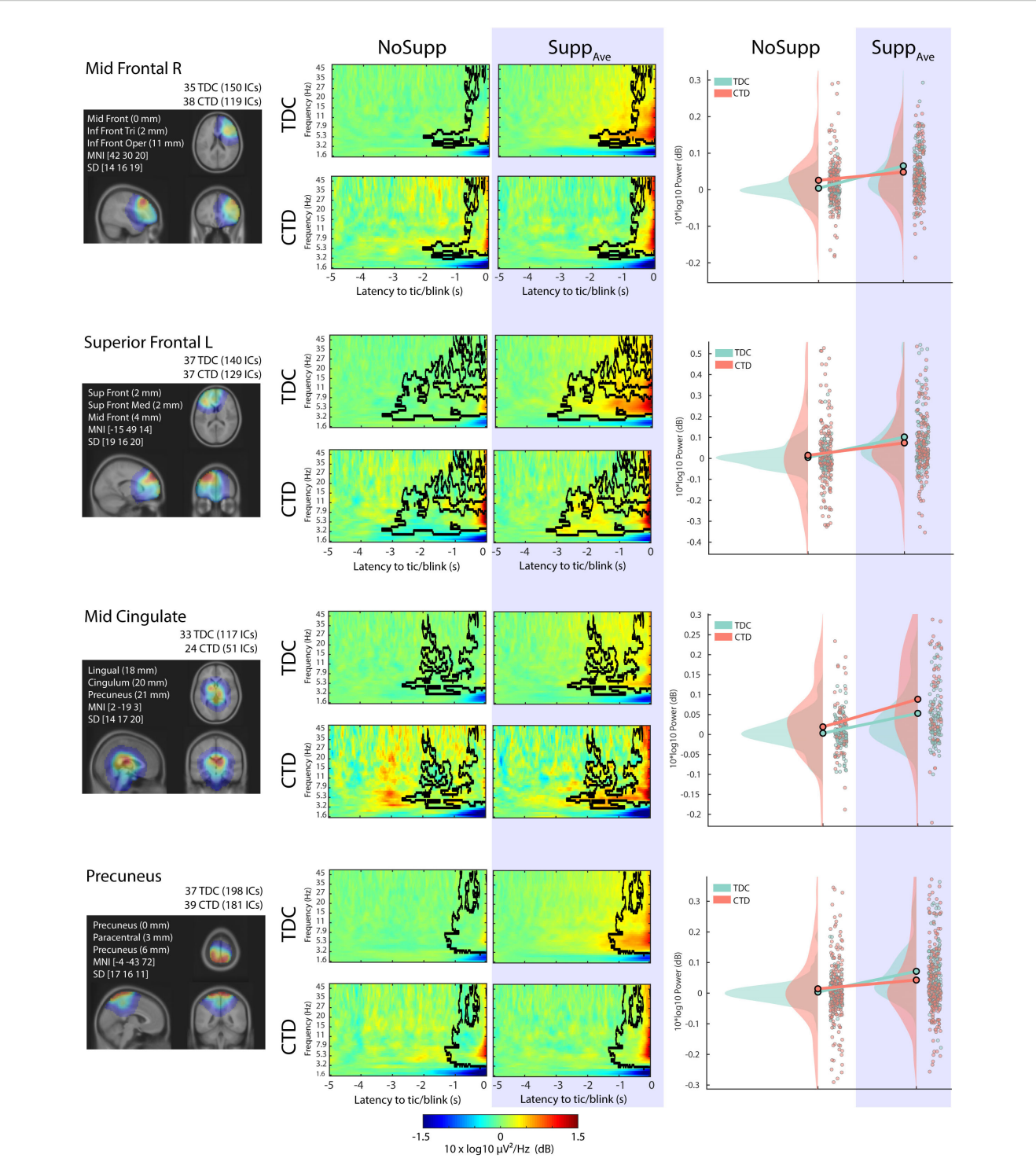
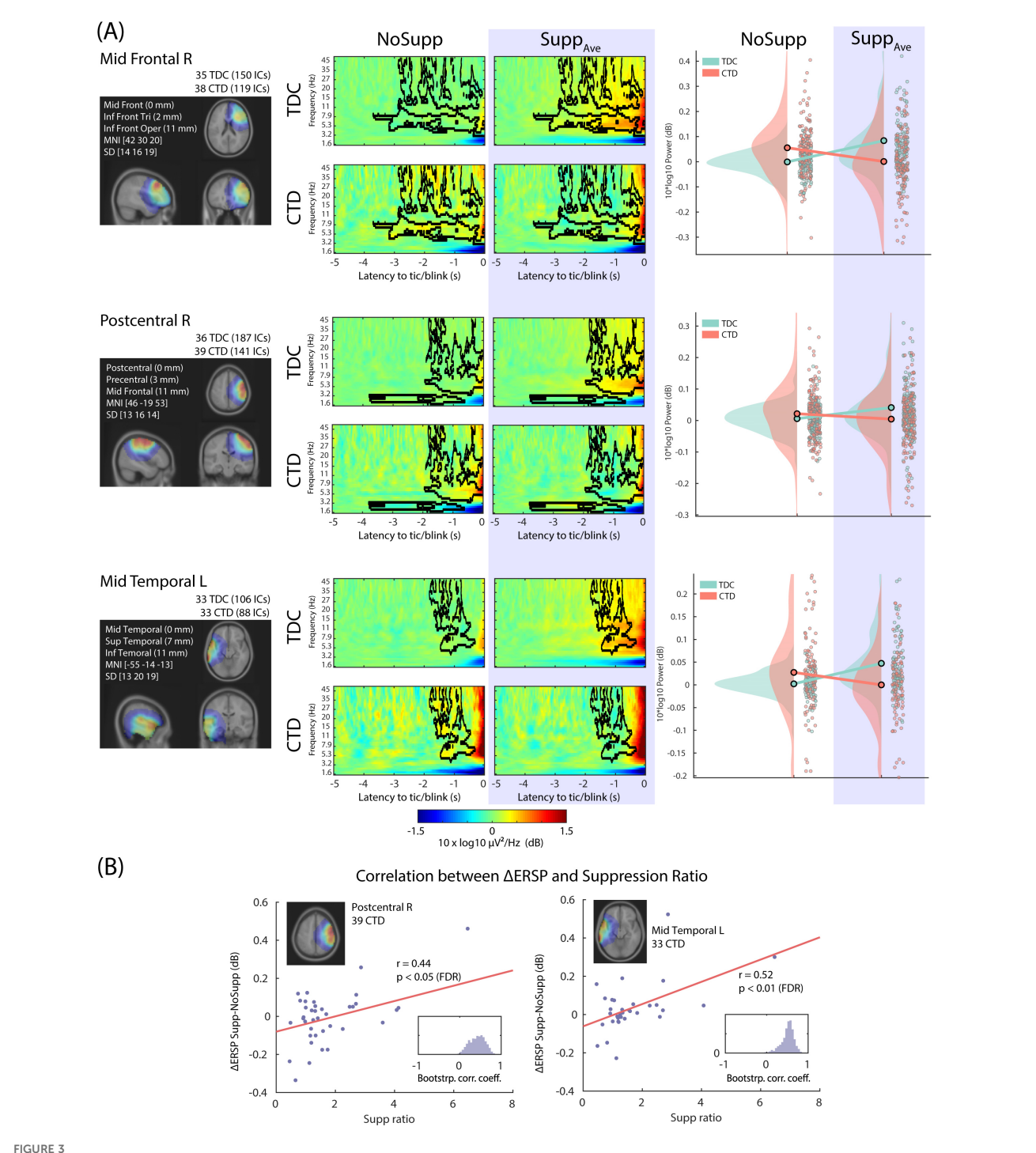


FIGURE 2
The four IC clusters that showed a main effect of Suppression, all of which showed a power increase during suppression. Left: The relative dipole density after applying 3-D Gaussian smoothing with FWHM 20 mm. Middle: The 2x2 event-related spectral perturbation (ERSP) plots. The baseline period was defined between -5 to -4 s relative to blink/tic onset. The black contour indicates the significance mask at p < 0.05 corrected for cluster-level family-wise error-rate (FWER) control. Right: The scatter plot and distribution of the mean value within the significance mask across ICs. TDC, typically developing children; CTD, chronic tic disorder.



The three IC clusters that showed interaction Suppression x Group, all of which showed suppression-related power decrease in CTD. (A) Left, the relative dipole density after applying the 3-D Gaussian smoothing with FWHM 20 mm. Middle, the 2x2 event-related spectral perturbation (ERSP) plots. The baseline period was defined between -5 to -4 s relative to blink/tic onset. The black contour indicates significance mask at p < 0.05 corrected for cluster-level family-wise error-rate (FWER) control. Right, the scatter plot and distribution of the mean value within the significance mask across ICs. (B) For the right postcentral and the left precentral/temporal IC clusters, the performance score of tic suppression (the horizontal axis, the higher the better) showed a positive correlation with relative EEG power increase during tic suppression compared with no suppression condition. The EEG power increase in these regions is the characteristic of control groups during blink suppression. TDC, typically developing children; CTD, chronic tic disorder.

remained significant (all $p < 6.17 \times 10^{-6}$) after separating the effect of Age and Drug. The effect of Age was significant for the superior frontal (p = 0.00254) and the precuneus (p = 0.00035) IC clusters. The effect of Drug was significant for the precuneus ($p = 6.29 \times 10^{-6}$). The adjusted R² ranged from 0.0554 to 0.111.

EEG data: interaction Suppression x Group

Out of the 13 IC clusters, 3 of them showed a significant interaction effect Suppression x Group, including 1 frontal and 2 central/temporal clusters (Figure 3). The right prefrontal IC cluster, which showed a similar power increase in both groups mainly in the theta-alpha range, now showed the opposite pattern in the beta range. These differential EEG power modulations across frequencies between the groups suggest the presence of abnormal beta-gamma EEG power modulation in the CTD. A similar pattern was found in the right central and left centro-temporal regions in broadband power (4 to 45 Hz), which indicates abnormal EEG power modulation in the bilateral sensorimotor regions.

The impact of Age and Drug was evaluated using the LME model including Age and Drug as fixed effect variables. For all the IC clusters shown in Figure 3, the interaction Suppression x Group remained significant (all p < 0.00166) after separating the effect of Age and Drug. The effect of Age was significant for the postcentral (p = 0.00211) IC cluster. The effect of Drug was significant for the postcentral (p = 0.000294) and the temporal (p = 0.000682). The adjusted R^2 ranged from 0.0426 to 0.0986.

Subsequently, we performed correlation analyses between the EEG power and the suppression performance. After applying the FDR correction across all the IC Clusters x Groups, only CTD in 2 IC clusters showed a significant result: better suppression in CTD was associated with increased power (i.e. ° Δ ERSP): r = 0.44 and 0.52 for the right central and the left centrotemporal ICs, respectively (p < 0.05 and p < 0.01, respectively, after FDR correction). Because TDC showed increased power during suppression, we interpreted the result that children with CTD with better suppression also showed more similar EEG power modulation to the TDC. We used the LME model to evaluate the impact of Age and Drug. For both IC clusters, the results from the correlation analysis remained significant (both p < 0.00618). The effect of Age did not reach significance (all p > 0.359). The effect of Drug was significant (p =0.0406 and 0.0408, respectively) but would not survive multiple comparison corrections.

Finally, we conducted correlation analyses between EEG power (NoSupp, Supp_{Ave}, and Δ ERSP i.e., NoSupp-Supp_{Ave}) and PUTS scores for each IC cluster. None of the results survived multiple comparison corrections using FDR. However, two IC clusters showed significant results only in Δ ERSP in uncorrected p-values: the left superior frontal cluster (Figure 2, the second row) showed r=0.357, p=0.028, and the left parieto-occipital cluster (not shown) showed r=0.427, p=0.009. These results may indicate preliminary EEG evidence of a link between premonitory urge and suppression-triggered EEG modulations.

Discussion

We performed independent component analysis (ICA)decomposed event-related potential analysis in the time-frequency domain to study brain dynamics during suppression of tic or blink using CTD and TDC subjects. We found three main results: (1) The main effect of Suppression was found in mostly frontal but also central regions reflected by power increase in the broad frequency band including the theta range, which indicates a common EEG signature between both groups; (2) an interaction effect of Suppression x Group was found in centro-temporal sensorimotor regions (in the broadband), as well as a frontal region (in the beta and gamma range) in which CTD showed power decrease while TDC showed power increase. Notably, there was a positive correlation between EEG power and performance in behavioral suppression in CTD, indicating that good suppressors in CTD show EEG power increase similar to TDC; (3) The effect of reward on tic suppression behavior was not significant.

Main effect of suppression

The main effect Suppression in both CTD and TDC was represented by an EEG power increase mainly in the theta band. We recently reported prefrontal EEG power increase during blink suppression in typically developing children (20). The current result extends the finding that this prefrontal theta power increase is probably a common EEG signature for tic suppression in CTD. The involvement of prefrontal regions, including the dorsolateral prefrontal cortex (DLPFC), in voluntary non-tic-related inhibition tasks (18, 19) as well as a tic inhibition task (16) confirms that our ICA-derived EEG sources activation in the time-frequency domain is in line with these neuroimaging studies. Thus, our results confirmed the expected engagement of the right prefrontal region in the task of tic suppression.

Another important region that showed up was the cingulate cortex. Care must be taken when interpreting the location of the IC cluster: the apparent location of the cluster centroid is in the subcortical region, but this is obviously due to the depth bias as mentioned before. When fitting a single equivalent current dipole model to a broad cortical source, the estimated location becomes deeper than the actual depth of such a layer of a dipole array. Distance-dependent attenuation of electric potential produced by a single dipole follows the inverse square law. However, the rate of the distance-dependent attenuation can be substantially mitigated by forming a widespread parallel dipole array (for more details, see Supplement 2 of Miyakoshi et al., (106)). Thus, we include a broader area of the cingulate cortex, including a posterior division of the anterior cingulate cortex (ACC) for the result interpretation. ACC has been associated with various types of urges such as itch (58), voiding of urine (59, 60), coughing (61, 62), and smoking (63). ACC is involved in subjective feeling, response coordination, selfmonitoring, assessment of motivational valence, and initiation of motor actions (64). ACC has been known to be a region where

regulatory and executive processes interact (65). Involvement of ACC was also reported in a previous blink suppression study (66) and anti-saccade study (67). One of the above cited studies concluded that bilateral dorsolateral prefrontal cortices and the anterior cingulate cortex are the key regions for suppression tasks for both children and adults (68), which is in line with the current result.

The anatomical and functional connection between the ACC and insula should be mentioned. Note that we do not intend to make a claim that any of our EEG results directly reflect insula activity, since epilepsy research indicated that scalp-recorded EEG cannot directly measure insula (69-72). However, it is obvious from neuroimaging studies that the insula is another central region involved in various kinds of suppression tasks, including blink (16, 17, 66, 73), air hunger (74), cough (75), and even the stop signal task in CTD (76). Both the ACC and insula are known to contain von Economo neurons (77) which are particularly large neurons unique to these regions and only found in great apes and humans. There is anatomical evidence that Brodmann area 24 has a reciprocal connection with the insular cortex (78, 79), which may be mediated by the von Economo neurons (80). There is additional evidence that the insula and midcingulate cortex, which represent limbic sensory and motor regions respectively, are the key network for motivation for action in urge (81). These M/ACC-insula connections may indicate an underlying anatomical structure that is indirectly reflected by the theta-band power increase we found in both groups in the cingulate cortex.

Interaction between suppression and group

In comparing CTD and TDC in tic or blink suppression, we found a group difference in the broadband power in the frontal and centro-temporal regions. We interpreted this centro-temporal area as representing sensorimotor regions. The involvement of the frontal region is discussed above, but notably this group-difference was found in the beta band. This may suggest there are differential EEG power modulations in non-overlapping frequency ranges between the groups: theta power changes are common, but beta power changes are the opposite between CTD and TDC. The involvement of sensorimotor regions in CTD has been reported in previous EEG studies (9, 82, 83). It is hypothesized that the inhibitory control exerted by frontal structures, such as the dorsolateral prefrontal cortex, inferior frontal gyrus, and supplementary motor area during voluntary movement and self-regulation, may be consistent with neural activity reported during tic inhibition and suppression (6, 84, 85). Furthermore, altered states and activities of the sensorimotor cortex in CTD were also reported by an MEG study (2) and TMS studies (3-5). These frontal and sensorimotor locations reported in the study of CTD are consistent with our findings. Furthermore, for the EEG power resolved at the bilateral sensorimotor areas, our results revealed that those children with CTD who could suppress the tics better showed greater increase in broadband power although the group tendency of CTD is the broadband power decrease. We interpret that the broadband power increases in the bilateral sensorimotor regions can be a neural marker that reflects the CTD children's ability to suppress tic. The time window of this broadband EEG modulation is about -2 to -1 sec until the suppression breaks and the movement begins. The time-frequency parameters of this important EEG marker were for the first time resolved spatiotemporally thanks to the EEG event-related potential paradigm.

The effect of reward in CTD

The facilitation of blink suppression by reward was only marginal in typically developing controls (TDC; p = 0.074) and absent in CTD ($p \approx 1$). This difference suggests reduced reward sensitivity in CTD. One likely reason is that, in our experimental design, rewards were delivered late and in bulk, rather than immediately and repeatedly at short intervals. The dopaminergic hyper-innervation hypothesis of CTD (86, 87) predicts that an elevated tonic dopamine level in CTD diminishes the impact of delayed, but less so for immediate, rewards. Consistent with this view, Greene and colleagues found that when children with CTD received a contingent reward after each 10-s tic-suppression block, performance improved markedly, whereas yoked, non-contingent rewards had little effect (23). Although we informed participants that the reward was contingent, its bulk, delayed delivery likely made it less effective for CTD. Thus, our interpretation is that elevated tonic dopamine level blunted the reward signal for bulk and delayed delivery in CTD.

Another possibility is that the effect of the EEG recording environment, such as wearing an electrode cap, may have disrupted tic and tic suppression behaviors and changed the CTD group's sensitivity to reward. Finally, the low base rate of tics in the NoSupp condition may have created a floor effect that negatively impacted the amount of decrease that was possible during the $Supp_{Rwd}$ condition.

Relation to neural network dysfunction associated with CTD

A translational study in transgenic mice demonstrated that a hyper-glutamatergic cortico-striato-pallido-thalamo-cortical (CSTC) loop can produce Tourette-like tics (88). In primates, the dorsal striatum, i.e., the putamen, receives dense glutamatergic input from frontal sensorimotor cortices (89–93). According to the hyper-glutamatergic CSTC model, excessive pyramidal drive from the motor cortex reaches the putamen (94–97), where more than 90% of neurons are GABAergic medium spiny neurons that project to the globus pallidus and substantia nigra (98). These output nuclei inhibit the anterior ventrolateral thalamus, whose efferents return to anterior M1 (99), completing a dysregulated feedback loop that favors tic generation. Human MRI work corroborates this circuitry, revealing putaminal and thalamic structural and tractographic abnormalities in CTD (100, 101). Consistent with these findings, our results identified a right post-

central sensorimotor component (Figure 2) whose activity scaled with voluntary tic suppression, and a mid-cingulate component that overlaps regions where gray-matter volume correlates with premonitory urges (100). Although scalp EEG cannot directly capture sub-cortical signals, anchoring analyses in the hyper-glutamatergic CSTC framework enables theory-driven interrogation of cingulate and sensorimotor oscillations as cortical read-outs of basal-ganglia dysfunction.

Implications for behavioral treatment

Comprehensive behavioral intervention for tics (CBIT) (102, 103) builds on habit reversal training (104, 105). Its success depends on trainee's ability to detect pre-monitory urges and to execute a voluntary counter-action, a process that recruits cingulosensorimotor circuits. Our data show recruitment of the midcingulate and sensorimotor cortices during instructed tic suppression, which are the key cortical nodes both for the CSTC model and the CBIT. These cortically contributed EEG signatures may serve as objective markers of therapeutic engagement. Future studies should examine whether CBIT modulates these EEG markers for normalization. Until such evidence is available, the present findings provide physiological support for the neural rationale underlying CBIT/HRT.

Limitations

We studied children with CTD, who may not be representative of adults with CTD due to potential developmental adaptations. Care must be taken when generalizing our results to adults with CTD. The same limitation applies to the difference between motor tics, which we focused on in this study, and vocal tics. Because of potential differences in neural mechanisms between the two types of tics, appropriate limitation must be added when generalizing the current results to the case of vocal tics.

We could use only about half of the CTD samples because the other half of the data sets did not meet inclusion criteria of minimum 15 trials per condition for 3 conditions. This could have excluded good tic suppressors from the final EEG analysis. When interpreting the obtained EEG results, we must take into consideration that the CTD data sets are biased towards poor suppressors. Finally, the gender balance in the CTD sample is biased towards male (27 males vs. 12 females). The effect of the interaction between CTD and gender imbalance is unknown. When interpreting the current results, this limitation should be considered.

Conclusion

We performed the first event-related potential analysis targeting suppression breaks to study the brain dynamics of the pre-tic or blink period. We found that both the CTD and TDC showed increased EEG power centered in the theta range in frontal, cingulate, and central regions. Meanwhile, we found that CTD showed a reversed pattern in broadband EEG power modulation in the centro-temporal sensorimotor regions. The regression analysis between this broadband power and suppression performance indicated a positive correlation in CTD, indicating that better tic suppression was associated with increased EEG power, similar to the TDC group during blink suppression. Thus, EEG power is a putative neural marker of tic suppression performance in CTD.

Data availability statement

The data that support the findings of this study are available from the senior author, SKL (Sloo@mednet.ucla.edu), and Matlab code is available from the corresponding author, MM, upon reasonable request following the completion of all necessary IRB-related registrations and approvals for data sharing.

Ethics statement

The studies involving humans were approved by University of California, Los Angeles (IRB number 13-00538). The studies were conducted in accordance with the local legislation and institutional requirements. Written informed consent for participation in this study was provided by the participants' legal guardians/next of kin.

Author contributions

MM: Formal analysis, Investigation, Methodology, Software, Writing – original draft, Writing – review & editing. JJ: Data curation, Investigation, Methodology, Software, Writing – review & editing. AD: Data curation, Investigation, Writing – review & editing. JP: Conceptualization, Investigation, Writing – review & editing. SM: Conceptualization, Methodology, Writing – review & editing. SKL: Conceptualization, Data curation, Funding acquisition, Investigation, Methodology, Project administration, Resources, Supervision, Writing – review & editing.

Funding

The author(s) declare financial support was received for the research and/or publication of this article. Funding for the current study was provided by National Institute of Mental Health R34MH101282, National Institute of Neurological Disorders and Stroke R01NS097484 and R01NS047293, National Institute of Child Health and Human Development R01HD108222; National Science Foundation BCS-2011716; The Swartz Center for Neural Computation, directed by Scott Makeig, was founded in 2001 by a generous gift from Dr. Jerome Swartz of The Swartz Foundation (Old Field, New York).

Conflict of interest

The authors declare that the research was conducted in the absence of any commercial or financial relationships that could be construed as a potential conflict of interest.

The author(s) declared that they were an editorial board member of Frontiers, at the time of submission. This had no impact on the peer review process and the final decision.

Generative AI statement

The author(s) declare that no Generative AI was used in the creation of this manuscript.

Any alternative text (alt text) provided alongside figures in this article has been generated by Frontiers with the support of artificial intelligence and reasonable efforts have been made to ensure accuracy, including review by the authors wherever possible. If you identify any issues, please contact us.

Publisher's note

All claims expressed in this article are solely those of the authors and do not necessarily represent those of their affiliated organizations, or those of the publisher, the editors and the reviewers. Any product that may be evaluated in this article, or claim that may be made by its manufacturer, is not guaranteed or endorsed by the publisher.

References

- 1. Morand-Beaulieu S, Grot S, Lavoie J, Leclerc JB, Luck D, Lavoie ME. The puzzling question of inhibitory control in Tourette syndrome: A meta-analysis. *Neurosci Biobehav Rev.* (2017) 80:240–62. doi: 10.1016/j.neubiorev.2017.05.006
- 2. Tinaz S, Belluscio BA, Malone P, van der Veen JW, Hallett M, Horovitz SG. Role of the sensorimotor cortex in Tourette syndrome using multimodal imaging. *Hum Brain Mapp.* (2014) 35:5834–46. doi: 10.1002/hbm.22588
- 3. Orth M, Münchau A, Rothwell JC. Corticospinal system excitability at rest is associated with tic severity in tourette syndrome. $Biol\ Psychiatry$. (2008) 64:248–51. doi: 10.1016/j.biopsych.2007.12.009
- 4. Orth M. Transcranial magnetic stimulation in Gilles de la Tourette syndrome. *J Psychosom Res.* (2009) 67:591–8. doi: 10.1016/j.jpsychores.2009.07.014
- 5. Orth M, Rothwell JC. Motor cortex excitability and comorbidity in Gilles de la Tourette syndrome. *J Neurol Neurosurg Psychiatr.* (2009) 80:29–34. doi: 10.1136/jnnp.2008.149484
- 6. Ganos C, Kahl U, Brandt V, Schunke O, Bäumer T, Thomalla G, et al. The neural correlates of tic inhibition in Gilles de la Tourette syndrome. *Neuropsychologia*. (2014) 65:297–301. doi: 10.1016/j.neuropsychologia.2014.08.007
- 7. Baym CL, Corbett BA, Wright SB, Bunge SA. Neural correlates of tic severity and cognitive control in children with Tourette syndrome. *Brain.* (2008) 131:165–79. doi: 10.1093/brain/awm278
- 8. Hong HJ, Sohn H, Cha M, Kim S, Oh J, Chu MK, et al. Increased frontomotor oscillations during tic suppression in children with Tourette syndrome. *J Child Neurol.* (2013) 28:615–24. doi: 10.1177/0883073812450317
- 9. Serrien DJ, Orth M, Evans AH, Lees AJ, Brown P. Motor inhibition in patients with Gilles de la Tourette syndrome: functional activation patterns as revealed by EEG coherence. *Brain.* (2005) 128:116–25. doi: 10.1093/brain/awh318
- 10. Duan K, Wu Q, Liao Y, Si Y, Bore JC, Li F, et al. Discrimination of Tourette syndrome based on the spatial patterns of the resting-state EEG network. *Brain Topogr.* (2021) 34:78–87. doi: 10.1007/s10548-020-00801-5
- 11. Morand-Beaulieu S, Wu J, Mayes LC, Grantz H, Leckman JF, Crowley MJ, et al. Increased alpha-band connectivity during tic suppression in children with Tourette syndrome revealed by source electroencephalography analyses. *Biol Psychiatry Cognit Neurosci Neuroimaging*. (2023) 8:241–50. doi: 10.1016/j.bpsc.2021.05.001
- 12. Morera Maiquez B, Jackson GM, Jackson SR. Examining the neural antecedents of tics in Tourette syndrome using electroencephalography. *J Neuropsychol.* (2022) 16:1–20. doi: 10.1111/jnp.12245
- 13. Zapparoli L, Macerollo A, Joyce EM, Martino D, Kilner JM. Voluntary tic suppression and the normalization of motor cortical beta power in Gilles de la Tourette syndrome: an EEG study. *Eur J Neurosci.* (2019) 50:3944–57. doi: 10.1111/ejn.14548
- 14. Peterson BS, Skudlarski P, Anderson AW, Zhang H, Gatenby JC, Lacadie CM, et al. A functional magnetic resonance imaging study of tic suppression in Tourette syndrome. *Arch Gen Psychiatry*. (1998) 55:326–33. doi: 10.1001/archpsyc.55.4.326
- 15. Kawohl W, Brühl A, Krowatschek G, Ketteler D, Herwig U. Functional magnetic resonance imaging of tics and tic suppression in Gilles de la Tourette syndrome. *World J Biol Psychiatry*. (2009) 10:567–70. doi: 10.1080/15622970802118356
- 16. van der Salm SMA, van der Meer JN, Cath DC, Groot PFC, van der Werf YD, Brouwers E, et al. Distinctive tics suppression network in Gilles de la Tourette syndrome distinguished from suppression of natural urges using multimodal imaging. *NeuroImage Clin.* (2018) 20:783–92. doi: 10.1016/j.nicl.2018.09.014

- 17. Berman BD, Horovitz SG, Morel B, Hallett M. Neural correlates of blink suppression and the buildup of a natural bodily urge. Neuroimage. (2012) 59:1441–50. doi: 10.1016/j.neuroimage. 2011.08.050
- 18. Aron AR, Robbins TW, Poldrack RA. Inhibition and the right inferior frontal cortex. *Trends Cognit Sci (Regul Ed)*. (2004) 8:170–7. doi: 10.1016/j.tics.2004.02.010
- 19. Aron AR, Robbins TW, Poldrack RA. Inhibition and the right inferior frontal cortex: one decade on. *Trends Cognit Sci (Regul Ed)*. (2014) 18:177–85. doi: 10.1016/j.tics.2013.12.003
- 20. Miyakoshi M, Jurgiel J, Dillon A, Chang S, Piacentini J, Makeig S, et al. Modulation of frontal oscillatory power during blink suppression in children: effects of premonitory urge and reward. *Cereb Cortex Commun.* (2020) 1:tgaa046. doi: 10.1093/texcom/tgaa046
- 21. Brandt VC, Beck C, Sajin V, Baaske MK, Bäumer T, Beste C, et al. Temporal relationship between premonitory urges and tics in Gilles de la Tourette syndrome. *Cortex.* (2016) 77:24–37. doi: 10.1016/j.cortex.2016.01.008
- 22. McGuire JF, Piacentini J, Scahill L, Woods DW, Villarreal R, Wilhelm S, et al. Bothersome tics in patients with chronic tic disorders: Characteristics and individualized treatment response to behavior therapy. *Behav Res Ther.* (2015) 70:56–63. doi: 10.1016/j.brat.2015.05.006
- 23. Greene DJ, Koller JM, Robichaux-Viehoever A, Bihun EC, Schlaggar BL, Black KJ. Reward enhances tic suppression in children within months of tic disorder onset. *Dev Cognit Neurosci.* (2015) 11:65–74. doi: 10.1016/j.dcn.2014.08.005
- 24. Woods DW, Himle MB. Creating tic suppression: comparing the effects of verbal instruction to differential reinforcement. *J Appl Behav Anal.* (2004) 37:417–20. doi: 10.1901/jaba.2004.37-417
- 25. Silverman WK, Albano AM. Anxiety Disorders Interview Schedule for DSM-IV: Parent Interview Schedule (Child Version). New York: Graywind Publications Inc (1996).
- 26. Kaufman J, Birmaher B, Brent D, Rao U, Flynn C, Moreci P, et al. Schedule for Affective Disorders and Schizophrenia for School-Age Children-Present and Lifetime Version (K-SADS-PL): initial reliability and validity data. *J Am Acad Child Adolesc Psychiatry*. (1997) 36:980–8. doi: 10.1097/00004583-199707000-00021
- 27. Leckman JF, Riddle MA, Hardin MT, Ort SI, Swartz KL, Stevenson J, et al. The Yale Global Tic Severity Scale: initial testing of a clinician-rated scale of tic severity. J Am Acad Child Adolesc Psychiatry. (1989) 28:566–73. doi: 10.1097/00004583-198907000-00015
- Scahill L, Riddle MA, McSwiggin-Hardin M, Ort SI, King RA, Goodman WK, et al. Children's Yale-Brown Obsessive Compulsive Scale: reliability and validity. J Am Acad Child Adolesc Psychiatry. (1997) 36:844–52. doi: 10.1097/00004583-199706000-00023
- 29. Woods DW, Piacentini J, Himle MB, Chang S. Premonitory Urge for Tics Scale (PUTS): initial psychometric results and examination of the premonitory urge phenomenon in youths with Tic disorders. *J Dev Behav Pediatr*. (2005) 26:397–403. doi: 10.1097/00004703-200512000-00001
- 30. Swanson JM, Schuck S, Porter MM, Carlson C, Hartman CA, Sergeant JA, et al. Categorical and dimensional definitions and evaluations of symptoms of ADHD: History of the SNAP and the SWAN rating scales. *Int J Educ Psychol Assess.* (2012) 10:51–70.
- 31. Achenbach TM, Ruffle TM. The Child Behavior Checklist and related forms for assessing behavioral/emotional problems and competencies. *Pediatr Rev.* (2000) 21:265–71. doi: 10.1542/pir.21-8-265

- 32. Gioia GA, Isquith PK, Retzlaff PD, Espy KA. Confirmatory factor analysis of the Behavior Rating Inventory of Executive Function (BRIEF) in a clinical sample. *Child Neuropsychol.* (2002) 8:249–57. doi: 10.1076/chin.8.4.249.13513
- 33. Wechsler D. Wechsler abbreviated scale of intelligence. San Antonio, TX: The Psychological Corporation (1999).
- 34. Delorme A, Makeig S. EEGLAB: an open source toolbox for analysis of single-trial EEG dynamics including independent component analysis. *J Neurosci Methods*. (2004) 134:9–21. doi: 10.1016/j.j.eumeth.2003.10.009
- 35. Plechawska-Wojcik M, Kaczorowska M, Zapala D. The artifact subspace reconstruction (ASR) for EEG signal correction. A comparative study. In: Świątek J, Borzemski L, Wilimowska Z, editors. Information systems architecture and technology: proceedings of 39th international conference on information systems architecture and technology ISAT 2018: part II Advances in intelligent systems and computing. Springer International Publishing, Cham. (2019) p. 125–35. doi: 10.1007/978-3-319-99996-8_12
- 36. Chang C-Y, Hsu S-H, Pion-Tonachini L, Jung T-P. Evaluation of artifact subspace reconstruction for automatic artifact components removal in multi-channel EEG recordings. *IEEE Trans BioMed Eng.* (2020) 67:1114–21. doi: 10.1109/TBME.2019.2930186
- 37. Blum S, Jacobsen NSJ, Bleichner MG, Debener S. A riemannian modification of artifact subspace reconstruction for EEG artifact handling. *Front Hum Neurosci.* (2019) 13:141. doi: 10.3389/fnhum.2019.00141
- 38. Chang C-Y, Hsu S-H, Pion-Tonachini L, Jung T-P. Evaluation of artifact subspace reconstruction for automatic EEG artifact removal. *Annu Int Conf IEEE Eng Med Biol Soc.* (2018) 2018:1242–5. doi: 10.1109/EMBC.2018.8512547
- 39. Gabard-Durnam LJ, Mendez Leal AS, Wilkinson CL, Levin AR. The Harvard automated processing pipeline for electroencephalography (HAPPE): standardized processing software for developmental and high-artifact data. Front Neurosci. (2018) 12:97. doi: 10.3389/fnins.2018.00097
- 40. Mullen TR, Kothe CAE, Chi YM, Ojeda A, Kerth T, Makeig S, et al. Real-time neuroimaging and cognitive monitoring using wearable dry EEG. *IEEE Trans BioMed Eng.* (2015) 62:2553–67. doi: 10.1109/TBME.2015.2481482
- 41. Miyakoshi M. Artifact subspace reconstruction (ASR): A candidate for a dream solution for EEG studies, sleep or awake. *Sleep*. (2023) 46:zsad241. doi: 10.1093/sleep/zsad241
- 42. Kothe CA, Makeig S. BCILAB: a platform for brain-computer interface development. *J Neural Eng.* (2013) 10:56014. doi: 10.1088/1741-2560/10/5/056014
- 43. Bell AJ, Sejnowski TJ. An information-maximization approach to blind separation and blind deconvolution. *Neural Comput.* (1995) 7:1129–59. doi: 10.1162/neco.1995.7.6.1129
- 44. Makeig S, Bell A, Jung T-P, Sejnowski T. Independent component analysis of electroencephalographic data. *Adv Neural Inf Process Syst.* (1996) 8:145–51.
- 45. Makeig S, Jung TP, Bell AJ, Ghahremani D, Sejnowski TJ. Blind separation of auditory event-related brain responses into independent components. *Proc Natl Acad Sci USA*. (1997) 94:10979–84. doi: 10.1073/pnas.94.20.10979
- 46. Makeig S, Westerfield M, Jung TP, Enghoff S, Townsend J, Courchesne E, et al. Dynamic brain sources of visual evoked responses. *Science*. (2002) 295:690–4. doi: 10.1126/science.1066168
- 47. Delorme A, Palmer J, Onton J, Oostenveld R, Makeig S. Independent EEG sources are dipolar. *PloS One.* (2012) 7:e30135. doi: 10.1371/journal.pone.0030135
- 48. Onton J, Makeig S. Information-based modeling of event-related brain dynamics. *Prog Brain Res.* (2006) 159:99–120. doi: 10.1016/S0079-6123(06)59007-7
- 49. Oostenveld R, Fries P, Maris E, Schoffelen J-M. FieldTrip: Open source software for advanced analysis of MEG, EEG, and invasive electrophysiological data. *Comput Intell Neurosci.* (2011) 2011:156869. doi: 10.1155/2011/156869
- 50. Piazza C, Miyakoshi M, Akalin-Acar Z, Cantiani C, Reni G, Bianchi AM, et al. An automated function for identifying EEG independent components representing bilateral source activity. In: Kyriacou E, Christofides S, Pattichis CS, editors. XIV Mediterranean Conference on Medical and Biological Engineering and Computing. Springer International Publishing, Cham (2016). p. 105–9. IFMBE Proceedings. doi: 10.1007/978-3-319-32703-7_22
- 51. Pion-Tonachini L, Kreutz-Delgado K, Makeig S. ICLabel: An automated electroencephalographic independent component classifier, dataset, and website. *Neuroimage*. (2019) 198:181–97. doi: 10.1016/j.neuroimage.2019.05.026
- 52. Rousseeuw PJ. Silhouettes: A graphical aid to the interpretation and validation of cluster analysis. *J Comput Appl Mathematics*. (1987) 20:53–65. doi: 10.1016/0377-0427 (87)90125-7
- 53. Groppe DM, Urbach TP, Kutas M. Mass univariate analysis of event-related brain potentials/fields I: a critical tutorial review. *Psychophysiology*. (2011) 48:1711–25. doi: 10.1111/j.1469-8986.2011.01273.x
- 54. Collins DL, Neelin P, Peters TM, Evans AC. Automatic 3D intersubject registration of MR volumetric data in standardized Talairach space. *J Comput Assist Tomogr.* (1994) 18:192–205. doi: 10.1097/00004728-199403000-00005
- 55. Lancaster JL, Woldorff MG, Parsons LM, Liotti M, Freitas CS, Rainey L, et al. Automated Talairach atlas labels for functional brain mapping. *Hum Brain Mapp*. (2000) 10:120–31. doi: 10.1002/1097-0193(200007)10:3<120::aid-hbm30>3.0.co;2-8
- 56. Li Y, Wang F, Liu J, Wen F, Yan C, Zhang J, et al. The correlation between the severity of premonitory urges and tic symptoms: A meta-analysis. *J Child Adolesc Psychopharmacol.* (2019) 29:652–8. doi: 10.1089/cap.2019.0048

- 57. Nunez PL, Srinivasan R. *Electric fields of the brain*. 198 Madison Avenue, New York, New York, 10016: Oxford University Press, Inc (2006). doi: 10.1093/acprof:oso/9780195050387.001.0001
- 58. Hsieh JC, Hägermark O, Ståhle-Bäckdahl M, Ericson K, Eriksson L, Stone-Elander S, et al. Urge to scratch represented in the human cerebral cortex during itch. *J Neurophysiol.* (1994) 72:3004–8. doi: 10.1152/jn.1994.72.6.3004
- 59. Kuhtz-Buschbeck JP, van der Horst C, Pott C, Wolff S, Nabavi A, Jansen O, et al. Cortical representation of the urge to void: a functional magnetic resonance imaging study. *J Urol.* (2005) 174:1477–81. doi: 10.1097/01.ju.0000173007.84102.7c
- 60. Griffiths D, Tadic SD, Schaefer W, Resnick NM. Cerebral control of the bladder in normal and urge-incontinent women. $Neuroimage.\ (2007)\ 37:1-7.\ doi: 10.1016/j.neuroimage.2007.04.061$
- 61. Mazzone SB, McLennan L, McGovern AE, Egan GF, Farrell MJ. Representation of capsaicin-evoked urge-to-cough in the human brain using functional magnetic resonance imaging. *Am J Respir Crit Care Med.* (2007) 176:327–32. doi: 10.1164/rccm.200612-18560C
- 62. Leech J, Mazzone SB, Farrell MJ. Brain activity associated with placebo suppression of the urge-to-cough in humans. *Am J Respir Crit Care Med.* (2013) 188:1069–75. doi: 10.1164/rccm.201306-1079OC
- 63. Brody AL, Mandelkern MA, Lee G, Smith E, Sadeghi M, Saxena S, et al. Attenuation of cue-induced cigarette craving and anterior cingulate cortex activation in bupropion-treated smokers: a preliminary study. *Psychiatry Res.* (2004) 130:269–81. doi: 10.1016/j.pscychresns.2003.12.006
- 64. Medford N, Critchley HD. Conjoint activity of anterior insular and anterior cingulate cortex: awareness and response. *Brain Struct Funct.* (2010) 214:535–49. doi: 10.1007/s00429-010-0265-x
- 65. Paus T. Primate anterior cingulate cortex: where motor control, drive and cognition interface. *Nat Rev Neurosci.* (2001) 2:417–24. doi: 10.1038/35077500
- 66. Lerner A, Bagic A, Hanakawa T, Boudreau EA, Pagan F, Mari Z, et al. Involvement of insula and cingulate cortices in control and suppression of natural urges. *Cereb Cortex.* (2009) 19:218–23. doi: 10.1093/cercor/bhn074
- 67. Milea D, Lehéricy S, Rivaud-Péchoux S, Duffau H, Lobel E, Capelle L, et al. Antisaccade deficit after anterior cingulate cortex resection. *Neuroreport.* (2003) 14:283–7. doi: 10.1097/00001756-200302100-00026
- 68. Mazzone L, Yu S, Blair C, Gunter BC, Wang Z, Marsh R, et al. An FMRI study of frontostriatal circuits during the inhibition of eye blinking in persons with Tourette syndrome. *Am J Psychiatry*. (2010) 167:341–9. doi: 10.1176/appi.ajp.2009.08121831
- 69. Isnard J, Guénot M, Sindou M, Mauguière F. Clinical manifestations of insular lobe seizures: a stereo-electroencephalographic study. *Epilepsia.* (2004) 45:1079–90. doi: 10.1111/j.0013-9580.2004.68903.x
- 70. Nguyen DK, Nguyen DB, Malak R, Leroux J-M, Carmant L, Saint-Hilaire J-M, et al. Revisiting the role of the insula in refractory partial epilepsy. *Epilepsia.* (2009) 50:510–20. doi: 10.1111/j.1528-1167.2008.01758.x
- 71. Desai A, Jobst BC, Thadani VM, Bujarski KA, Gilbert K, Darcey TM, et al. Stereotactic depth electrode investigation of the insula in the evaluation of medically intractable epilepsy. *J Neurosurg.* (2011) 114:1176–86. doi: 10.3171/2010.9.JNS091803
- 72. Ryvlin P, Picard F. Invasive investigation of insular cortex epilepsy. J Clin Neurophysiol. (2017) 34:328–32. doi: 10.1097/WNP.000000000000395
- 73. Berman BD, Horovitz SG, Hallett M. Modulation of functionally localized right insular cortex activity using real-time fMRI-based neurofeedback. *Front Hum Neurosci.* (2013) 7:638. doi: 10.3389/fnhum.2013.00638
- 74. Banzett RB, Mulnier HE, Murphy K, Rosen SD, Wise RJ, Adams L. Breathlessness in humans activates insular cortex. *Neuroreport*. (2000) 11:2117–20. doi: 10.1097/00001756-200007140-00012
- 75. Mazzone SB, Cole LJ, Ando A, Egan GF, Farrell MJ. Investigation of the neural control of cough and cough suppression in humans using functional brain imaging. *J Neurosci.* (2011) 31:2948–58. doi: 10.1523/JNEUROSCI.4597-10.2011
- 76. Fan S, Cath DC, van der Werf YD, de Wit S, Veltman DJ, van den Heuvel OA. Trans-diagnostic comparison of response inhibition in Tourette's disorder and obsessive-compulsive disorder. *World J Biol Psychiatry.* (2018) 19:527–37. doi: 10.1080/15622975.2017.1347711
- 77. Allman JM, Tetreault NA, Hakeem AY, Manaye KF, Semendeferi K, Erwin JM, et al. The von Economo neurons in frontoinsular and anterior cingulate cortex in great ages and humans. *Brain Struct Funct.* (2010) 214:495–517. doi: 10.1007/s00429-010-0254-0
- 78. Mesulam MM, Mufson EJ. Insula of the old world monkey. III: Efferent cortical output and comments on function. *J Comp Neurol.* (1982) 212:38–52. doi: 10.1002/cne.902120104
- 79. Vogt BA, Pandya DN. Cingulate cortex of the rhesus monkey: II. Cortical afferents. J Comp Neurol. (1987) 262:271–89. doi: 10.1002/cne.902620208
- 80. Craig ADB. How do you feel-now? The anterior insula and human awareness. Nat Rev Neurosci. (2009) 10:59–70. doi: 10.1038/nrn2555
- 81. Jackson SR, Parkinson A, Kim SY, Schüermann M, Eickhoff SB. On the functional anatomy of the urge-for-action. *Cognit Neurosci.* (2011) 2:227–43. doi: 10.1080/17588928.2011.604717
- 82. Thibault G, O'Connor KP, Stip E, Lavoie ME. Electrophysiological manifestations of stimulus evaluation, response inhibition and motor processing in

Tourette syndrome patients. Psychiatry Res. (2009) 167:202-20. doi: 10.1016/j.psychres.2008.03.021

- 83. Yordanova J, Heinrich H, Kolev V, Rothenberger A. Increased event-related theta activity as a psychophysiological marker of comorbidity in children with tics and attention-deficit/hyperactivity disorders. *Neuroimage*. (2006) 32:940–55. doi: 10.1016/j.neuroimage.2006.03.056
- 84. Deckersbach T, Chou T, Britton JC, Carlson LE, Reese HE, Siev J, et al. Neural correlates of behavior therapy for Tourette's disorder. *Psychiatry Res.* (2014) 224:269–74. doi: 10.1016/j.pscychresns.2014.09.003
- 85. Roessner V, Overlack S, Schmidt-Samoa C, Baudewig J, Dechent P, Rothenberger A, et al. Increased putamen and callosal motor subregion in treatment-naïve boys with Tourette syndrome indicates changes in the bihemispheric motor network. *J Child Psychol Psychiatry*. (2011) 52:306–14. doi: 10.1111/j.1469-7610.2010.02324.x
- 86. Maia TV, Conceição VA. Dopaminergic disturbances in tourette syndrome: an integrative account. *Biol Psychiatry*. (2018) 84:332–44. doi: 10.1016/j.biopsych.2018.02.1172
- 87. Maia TV, Conceição VA. The roles of phasic and tonic dopamine in tic learning and expression. *Biol Psychiatry*. (2017) 82:401–12. doi: 10.1016/j.biopsych.2017.05.025
- 88. Nordstrom EJ, Bittner KC, McGrath MJ, Parks CR, Burton FH. Hyperglutamatergic cortico-striato-thalamo-cortical circuit" breaker drugs alleviate tics in a transgenic circuit model of Tourette's syndrome. *Brain Res.* (2015) 1629:38–53. doi: 10.1016/j.brainres.2015.09.032
- 89. Yeterian EH, Van Hoesen GW. Cortico-striate projections in the rhesus monkey: the organization of certain cortico-caudate connections. *Brain Res.* (1978) 139:43–63. doi: 10.1016/0006-8993(78)90059-8
- 90. Wilson CJ, Groves PM. Spontaneous firing patterns of identified spiny neurons in the rat neostriatum. *Brain Res.* (1981) 220:67–80. doi: 10.1016/0006-8993(81)90211-0
- 91. Alexander GE, DeLong MR, Strick PL. Parallel organization of functionally segregated circuits linking basal ganglia and cortex. *Annu Rev Neurosci.* (1986) 9:357–81. doi: 10.1146/annurev.ne.09.030186.002041
- 92. Albin RL, Young AB, Penney JB. The functional anatomy of basal ganglia disorders. $Trends\ Neurosci.\ (1989)\ 12:366-75.\ doi: 10.1016/0166-2236(89)90074-x$
- 93. Haber SN, Knutson B. The reward circuit: linking primate anatomy and human imaging. Neuropsychopharmacology. (2010) 35:4–26. doi: 10.1038/npp.2009.129
- 94. Wang Z, Maia TV, Marsh R, Colibazzi T, Gerber A, Peterson BS. The neural circuits that generate tics in Tourette's syndrome. *Am J Psychiatry*. (2011) 168:1326–37. doi: 10.1176/appi.ajp.2011.09111692

- 95. Neuner I, Werner CJ, Arrubla J, Stöcker T, Ehlen C, Wegener HP, et al. Imaging the where and when of tic generation and resting state networks in adult Tourette patients. Front Hum Neurosci. (2014) 8:362. doi: 10.3389/fnhum.2014.00362
- 96. Worbe Y, Marrakchi-Kacem L, Lecomte S, Valabregue R, Poupon F, Guevara P, et al. Altered structural connectivity of cortico-striato-pallido-thalamic networks in Gilles de la Tourette syndrome. *Brain*. (2015) 138:472–82. doi: 10.1093/brain/awu311
- 97. Shitova AD, Zharikova TS, Kovaleva ON, LuChina AM, Aktemirov AS, Olsufieva AV, et al. Tourette syndrome and obsessive-compulsive disorder: A comprehensive review of structural alterations and neurological mechanisms. *Behav Brain Res.* (2023) 453:114606. doi: 10.1016/j.bbr.2023.114606
- 98. Haber SN. Corticostriatal circuitry. Dialogues Clin Neurosci. (2016) 18:7–21. doi: 10.31887/DCNS.2016.18.1/shaber
- 99. Jones EG ed. *The Thalamus*. New York: Plenum Press (1985). doi: 10.1007/978-1-4615-1749-8
- 100. Jackson SR, Sigurdsson HP, Dyke K, Condon M, Jackson GM. The role of the cingulate cortex in the generation of motor tics and the experience of the premonitory urge-to-tic in Tourette syndrome. *J Neuropsychol.* (2021) 15:340–62. doi: 10.1111/jnp.12242
- 101. Hsu C-J, Wong LC, Wang H-P, Chung Y-C, Kao T-W, Weng C-H, et al. The microstructural change of the brain and its clinical severity association in pediatric Tourette syndrome patients. *J Neurodev Disord*. (2023) 15:34. doi: 10.1186/s11689-023-09501-0
- 102. Woods DW, Piacentini J, Chang S, Deckersbach T, Ginsburg G, Peterson A, et al. Managing Tourette Syndrome: A Behavioral Intervention for Children and Adults Therapist Guide (Treatments That Work). Ist ed. Oxford: Oxford University Press (2008).
- 103. Piacentini J, Woods DW, Scahill L, Wilhelm S, Peterson AL, Chang S, et al. Behavior therapy for children with Tourette disorder: a randomized controlled trial. JAMA. (2010) 303:1929–37. doi: 10.1001/jama.2010.607
- 104. Azrin NH, Nunn RG. Habit-reversal: a method of eliminating nervous habits and tics. Behav Res Ther. (1973) 11:619–28. doi: 10.1016/0005-7967(73)90119-8
- 105. Cook CR, Blacher J. Evidence-based psychosocial treatments for tic disorders. Clin Psychol Sci Pract. (2007) 14:252–67. doi: 10.1111/j.1468-2850.2007.00085.x
- 106. Miyakoshi M, Gehrke L, Gramann K, Makeig S, Iversen J. The AudioMaze: An EEG and motion capture study of human spatial navigation in sparse augmented reality. *Eur J Neurosci.* (2021) 54:8283–307. doi: 10.1111/ejn.15131